Thermo-mechanical behaviour of composite moulding compounds at elevated temperatures

Zoltan J. Gombos [*], Paul McCutchion, Luke Savage

Exeter Advanced Technologies, University of Exeter, Exeter, EX4 4QF, United Kingdom

A B S T R A C T

The use of fibre-reinforced polymer composites as a lightweight metal replacement for automotive componentry is constantly expanding into new and more challenging application areas (e.g. whole range of under-bonnet, exhaust applications and other automotive components), where service temperatures are not expected to go beyond 150 °C. This study seeks to provide some useful baseline data on the bending stiffness performance of a large range of commercially available composite moulding compounds, in order to provide guidance in selecting appropriate materials for various applications requiring higher operating temperatures, where retention of bending stiffness is a key parameter. Whilst glass transition data can give some indication, this study seeks to go further. Three point bending flexural tests and Dynamic Mechanical Analysis were used to investigate and compare properties both at ambient and 150 °C comparing various composite systems, particularly phenolics, one of the fastest-growing systems in the thermoset moulding compounds market.

1. Introduction

Polymer matrix composite materials offer a cheap and lightweight alternative to metal componentry and now feature as part of the primary load-bearing structures in military and commercial aviation aircraft [1]. There is now a desire to expand usage further, into more harsh environments where a greater degree of thermal resistance is required. The aviation industry has driven the research agenda that in turn, has helped lead to the development of a whole range of specialist resin systems for high temperature including bis-male-imides (BMI), polyimides, cyanates, liquid crystalline polymers, and their composites [2]. Furthermore, the whole poly-aryl-ether-ketone (PAEK) family, which includes poly-ether-ether- ketone (PEEK) and poly-ether-ketone-ketone (PEKK) and their composites are widely used in aerospace applications due to the inherent weight saving, chemical and thermal resistance, and mechanical performance [3]. Whilst some of these grades can withstand sustained thermal excursions in the region of 400 °C, there are also difficulties. These materials require complex and lengthy processing operations, and are high cost. These factors preclude their use for high volume componentry, such as those required by mainstream automotive applications. Whilst the use of conventional thermoset composites is well established in aviation, the automotive industry represents the next sector with huge growth potential for composites. However the two

sectors differ in that mainstream automotive applications typically require production run numbers in to the 100,000s. Consequentially, polymer composite compression moulding compounds and composite injection moulding grades are the main two types of composite systems/manufacturing techniques most exploited for automotive applications.

This study focuses on the viability of using moulding compounds for application in higher temperature environments up to 150 °C, such as the engine compartment, manifolds covers, battery boxes, ducting, exhaust and other automotive components, which are now prime targets for composites as lightweight metal replacements [4–6]. Indeed, polymer composites are even being considered for the engine cylinder block itself [7]. Past studies of high temperature mechanical performance of polymeric composites have been driven by requirements for fire protection where heat transfer models were developed for vinyl-esters [8]. Other groups have sought to develop models for compression moulded composites that aim to predict thermo-mechanical behaviour, together with the effects of fibre orientation in compression moulded composite parts [9]. The thermomechanical performance of phenolic, polyester and epoxy composites and how they disintegrate at high temperatures has also attracted much attention in relation to their use as possible ablation materials for space/ballistic applications [10–16]. Several research programmes have sought to further improve the thermal

---

* Corresponding author.
  E-mail address: z.j.gombos@exeter.ac.uk (Z.J. Gombos).

stability of phenolics by using nanoparticles [17,18]. This study however, focuses on the retention of bending stiffness through more modest temperature rises, and focuses particularly on phenolic moulding compounds, as these are known to exhibit outstanding thermal performance and are of low cost [19–22]. Both glass and carbon fibre reinforced materials were used in this study to cover the commercially available range of moulding compounds. Although the higher cost of the carbon fibre is still one of the largest hurdles to production implementation within the automotive industry [23,24] where carbon fibre grades are used only when their low density and exceptional stiffness are required and the application can justify the higher cost. Carbon fibre grades are also sometimes favoured because of their electrical properties [25], such as energy storage [26], or even protection against lightning strikes [27]. Cost however remains a barrier widespread application. To address this issue, some research has been carried out aiming to lower the carbon fibre cost by e.g. using lignin precursor, which reduces the cost by around 50% compared to the commercial PAN precursor based fibres [28,29]. Recycled carbon fibre has also been considered in thermoset based Sheet Moulding Compounds [30] or in thermoplastics, such as PEEK [31] in order to lower the cost. The relative price of carbon fibre composites can also be dramatically reduced if hybrid systems (glass-/carbon) are used due to adding carbon fibre into glass reinforced composites increases the flexural modulus significantly when carbon fibres are situated close to the specimen surfaces [32]. These initiatives might further assist the mainstream use of carbon fibre in automotive industry.

A range of commercial phenolic moulding compounds are assessed, firstly using a Dynamic Mechanical Analysis (DMA), a widely used testing method to characterise the thermo-mechanical properties of various heat resistant polymer systems [33–37]. Samples of moulded composite were tested between ambient and 150 °C, where bending stiffness is assessed using the standard three point bending test set up. Uniquely, these DMA results are then compared to full scale standard flexural performance, where three point flexural tests are performed both at ambient and at 150 °C. This study assesses the performance of the phenolic moulding compounds compared to the several other commercially available moulding compounds. The most commonly used resins in Sheet Moulding Compounds (SMC) used in compression moulding operations are polyester, vinyl-ester, epoxy and phenolic [38]. However, other types of resin systems with excellent heat resistant properties can also be used in compression moulding, such as

bis-male-imides (BMI) and polyether-ether-ketone (PEEK). Furthermore various grades of epoxy-based discontinuous aligned fibre tapes are suitable for compression moulding, with a representative example included in this study [39,40]. The aim is to provide a valuable data set that goes beyond the information available from manufacturers' datasheets, or available in reference texts but would be an absolute requirement, as a materials selection criteria, for automotive designers.

2. Experiments

2.1. Materials and methodology

In this study various types of commercially available moulding compounds were used with a special focus on heat resistant phenolic based resin systems, which can operate at elevated temperatures. This temperature was chosen at 150 °C because it represents the maximum likely operating temperature in many automotive applications. The main properties of the composite moulding compounds used in this work are listed in Table 1. The materials were selected in order to cover many of the heat resistant resins (phenolic, polyimide, PEEK) and fibres (glass, carbon) available to date. The fibre forms are varied from chopped granulate with mineral fillers, sheet moulding compounds (SMC), pre impregnated rovings and continuous orthogonally woven prepreg. According to the different composite systems examined, the fibre lengths cover a large range: 3–6; 12.5; 25; 50 mm and continuous, while the fibre ratio varied between 35 and 81 wt%. Both Novolac and accelerated Resole type of phenolic moulding compounds were used in this study. The selected bis-male-imide (BMI) and polyether-ether-ketone (PEEK) based materials are mainly used in aerospace applications due to the higher price of the raw materials and extra cost of processing. Therefore their application in automotive industry is limited at the moment but data is provided for comparison. Vinyl-ester and epoxy based moulding compounds were tested and the data also used for comparison.

2.2. Sample preparation

This research focuses on composite moulding compounds, therefore compression moulding was selected accordingly. This manufacturing process offers fast processing time with relatively low operation cost.

Table 1
Identification of the composite moulding compounds, their main properties and processing parameters.

Material	Resin	Fibre reinforcement	Fibre length	Density (g/cm³)	Process	Moulding Temperature (°C)/Pressure (MPa)/Time (min)
PH1A[a]	Phenolic (Novolac)	Glass, 35 wt% (Chopped)	3–6 mm	2.05	Injection moulding	170/>15/0.6
PH1B[a]	Phenolic (Novolac)	Glass, 35 wt% (Chopped)	3–6 mm	2.05	Compression moulding	170/9.6/3
PH2	Phenolic (Resole)	Glass, 40 wt% (SMC)	25 mm	1.78	Compression moulding	145/3.8/15
PH3	Phenolic (Resole)	Glass, 81 wt% (Woven)	Continuous	2.10	Compression moulding	145/1.3/15
PH4	Phenolic (Resole)	Glass, 40 wt% (Rovings)	25 mm	1.79	Compression moulding	170/18/10
PH5	Phenolic (Resole)	Carbon, 45 wt% (SMC)	25 mm	1.55	Compression moulding	160/7.1/6
VE1	Vinyl-ester	Glass, 52 wt% (SMC)	25 mm	1.71	Compression moulding	150/4.0/3
VE2	Vinyl-ester	Carbon, 40 wt% (SMC)	25 mm	1.42	Compression moulding	150/4.0/3
VE3	Vinyl-ester	Glass, 60 wt% (SMC)	12.5 mm	1.89	Compression moulding	150/7.1/4
EP	Epoxy	Carbon, 48 wt% (SMC)	25 mm	1.54	Compression moulding	130/8.5/30
BMI	Bis-male-imide	Carbon, 52 wt% (Rovings)	50 mm	1.44	Compression moulding	200/20/90
PEEK	Polyether-ether-ketone	Carbon, 50 wt% (Rovings)	25 mm	1.56	Compression moulding	400/7.9/10

a PH1A and PH1B are the same material but moulded with different technique.

$4 \times 230 \times 230$ mm composite panels were compression moulded with an 800 kN (equals 15 MPa for the area specified) maximum capacity Bytec (ser. no. A10421) hydraulic press. Some materials (PH4, BMI) require higher processing pressure than the mentioned set-up could offer. Consequently a $4 \times 100 \times 100$ mm mould tool was used in those cases to achieve pressures over 15 MPa. The PEEK panels were also prepared in the smaller mould tool and by using a Lab Tech LP-S-50 (ser. no. 1310–50) hydraulic press due to the higher material processing temperature (400 °C) required. The disadvantage of using the smaller mould was that the specimens were machined only in one direction (see Fig. 1b). However, DMA specimens were still cut in two orthogonal directions for checking any orientation effected behaviour. The processing parameters were set according to data obtained from materials datasheets and provided by material suppliers. For mould release Kömmerling Cilrelease 393, Loctite Frekote 700-NC and Tygris Ceramic release agent IS35 were used for phenolics/BMI, vinyl-ester/epoxy and PEEK, respectively. PH1A and PH1B has release agent included to the formulation (proprietary) and therefore did not need any additional application in the mould. After the moulding process, the panels were then allowed to cool to room temperature before any further preparation. The flexural test and DMA samples from the $4 \times 230 \times 230$ mm composite panels were machined on Haas VF-I CNC machine (ser. no. 1480) with a Titanium carbide 3 mm diameter milling tool in two orthogonal directions (X and Y) to check any inhomogeneity within the moulded panels (Fig. 1a). The specimens from the $4 \times 100 \times 100$ mm composite panels (Fig. 1b) were cut using Buehler Isomet low speed cutter (model no. 11-1280-250, ser.no. 657-ISF-5674) assembled with a 4" diameter x 0.3 mm thickness impregnated diamond cutting blade (PI-KEM Ltd, P15016). The nominal dimensions of the specimens were $4 \times 15 \times 80$ mm and $2 \times 5 \text{x} 45$ mm for flexural and DMA tests according to ISO 14125 and ISO 6721 standards, respectively. A 16 h post-curing process was applied at 180 ± 2 °C in a Genlab N200F (ser.no. YIE118) air circulation laboratory oven on a series of phenolic samples. This temperature was chosen because it is a standard post-curing temperature used in the automotive industry [34,41].

2.3. Flexural tests (three point bending)

The flexural tests were carried out with Lloyds EZ 20 (ser. no. 102671) universal testing machine equipped with a 10 kN load cell with 0.5% accuracy grade (ser. no. 015029). The samples were tested as Class II materials according to ISO 14125 standard, which applies to plastics reinforced with mats, continuous matting and fabrics, as well as mixed formats, such as bulk (BMC), sheet (SMC) moulding compounds and glass mat reinforced thermoplastics (GMT). Therefore the test

parameters selected were 64 mm outer span length and 2 mm/min test speed to comply with a 1% strain rate. The tests were carried out at room temperature (23 ± 2 °C) and also at elevated temperature (150 ± 2 °C) in a temperature controlled TC 550 (ser. no. TS 363) heated chamber. Five specimens were tested in each of the two orthogonal (X and Y) directions both at ambient and at 150 °C, cut from the $4 \times 230 \times 230$ mm panels. In case of the samples cut in one direction from the $4 \times 100 \times 100$ mm panels, six-six specimens were tested in ambient and 150 °C. The specimens marked with odd numbers were used at ambient (X1 … X9 and Y1⋯Y9), while the samples marked with even numbers were tested at 150 °C (X2 … X10 and Y2⋯Y10). In this way the effect of any material property variation within the composite panels could be assessed.

2.4. Dynamical mechanical analysis (DMA)

The dynamic mechanical tests were performed using a Mettler Toledo DMA1 (ser. no. B350116591) dynamic mechanical analyser. The data was collected and analysed by using STARe software. In this study, the specimens were deformed under flexural cyclic load using a three point bending arrangement with 30 mm span length. This set-up is common for testing composites with high stiffness values and the test results can be compared with the data obtained from the flexural tests. The DMA tests were carried out in a fixed-frequency mode in which the frequency was held constant at 1 Hz, whilst the amplitude was set to 10 μm and the temperature was ramped from 20 °C to 200 °C at a heating rate of 3 °C/min. Specimens were tested in two orthogonal (X and Y) directions.

2.5. Micro computed tomography

The fibre orientation of the cured moulding compound specimens were analysed with micro computed tomography (micro-CT). The DMA samples were scanned using X-Tek Benchtop CT 160 Xi (X-Tek Systems Ltd/Nikon Metrology UK Ltd, England) with the following scanning conditions: voltage of 70 kV, current of 60 μA, voxel size of 38.7 μm for overall and 7.1 μm for close up images with 360° rotation. The scanned images were processed with VGStudio MAX 2.1 software.

3. Results and discussion

3.1. Flexural (three point bending) test results

During three point bending the specimen experiences a complex combination of stresses. The upper surface of the specimen is exposed to compression during loading the lower surface is under tension, whilst shear forces develop within the material between the supports. The main focus of this research was to establish data for the retained stiffness of the materials at the selected higher operating temperature (150 °C). In other words how the materials perform at 150 °C relative to room temperature performance. This parameter (referred to as retained flexural modulus in this study) was obtained by Eq. (1).

$$E_{f,\ retained} = \frac{E_{f\ @150°C}}{E_{f\ @RT}} \tag{1}$$

The flexural properties of the moulded and moulded than post-cured samples are summarised in Fig. 2. More detailed information reported in Table 2 for moulded, and in Table 3 for post-cured phenolic samples. It should be noted that data presented in this work were derived from 2D randomised quasi-isotropic samples based on the fact that there is no significant difference of the mechanical properties in the two orthogonal directions, which accounts for some of the divergence from idealised (aligned) mechanical property values presented in several manufacturers datasheets. Here follows a general discussion of the results, together with some further explanation of the results presented.
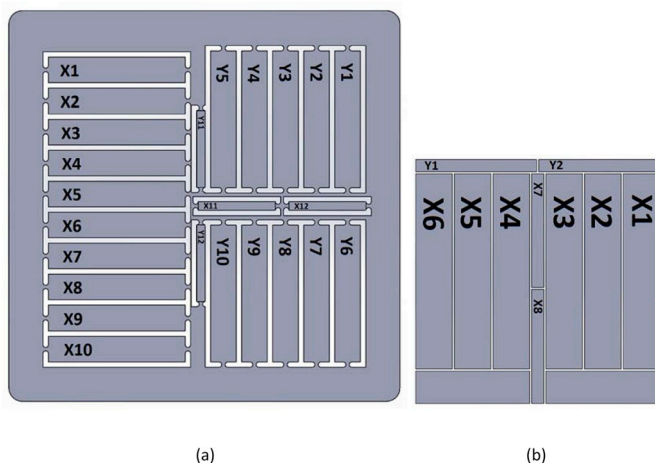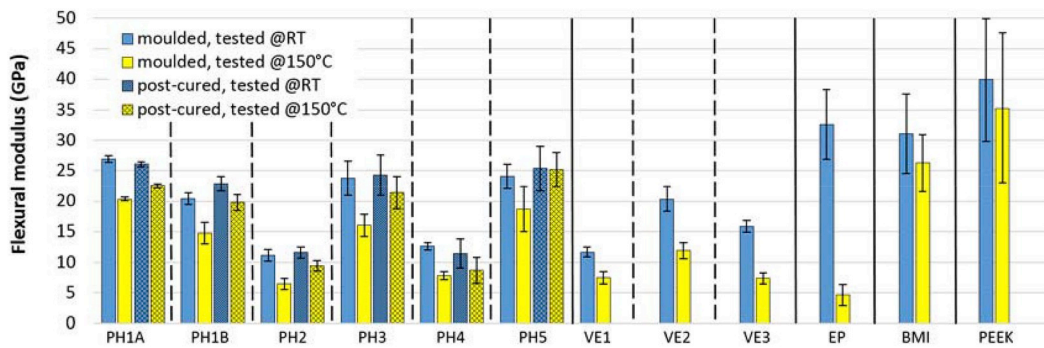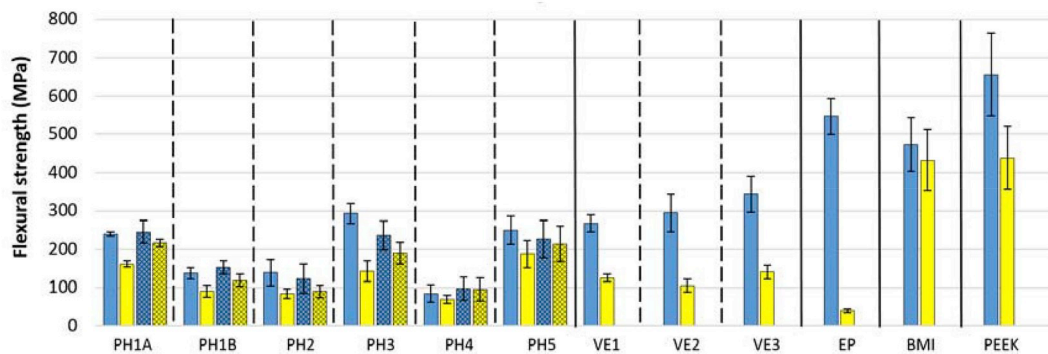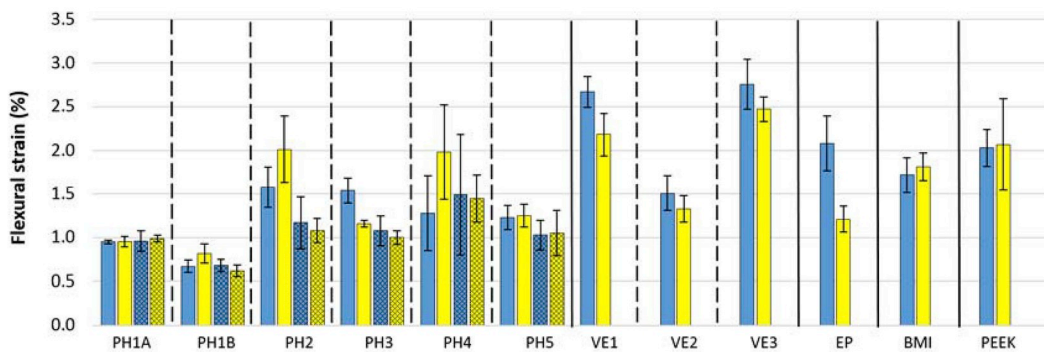

Fig. 1. Specimen machining plan from $4 \times 230 \times 230$ mm (a) and $4 \times 100 \times 100$ mm (b) composite panels.

(a)

(b)

(c)

Fig. 2. Flexural properties of the moulded samples at room temperature (RT) and elevated temperature (150 °C), grouped by resin types, flexural modulus (a), flexural strength (b) and flexural strain at failure (c), for phenolic samples the moulded and post-cured results also included.

3.1.1. Compression moulded specimens

Firstly it is important to note that although processing methods were kept constant for most materials (compression moulding with $4 \times 230 \times 230$ mould tool, which facilitated test specimens to be cut from 2 directions in the mould), there were some variations from this due to particular requirements of some of the materials. For PH4, BMI and PEEK a smaller mould tool was used as these samples required higher

processing pressure or temperature. This tool size allowed for test specimens to be cut out in one direction only.

A review of the data shows that PH1B, which contains a substantial amount of mineral filler, has a flexural modulus over 80% higher compared to PH2, which consisted of similar glass fibre content but longer fibre length without any filler. PH1B failed at below 1% flexural strain, compared to PH2, which withstood around 2% flexural strain.

Table 2
Flexural properties of the moulded samples in two orthogonal directions*.

Material	E_f data (GPa)	E_f at RT (GPa)	E_f at 150 °C (GPa)	E_f retained (%)	σ_{fM} data (MPa)	σ_{fM} at RT (MPa)	σ_{fM} at 150 °C (MPa)	ε_{fM} at RT (%)	ε_{fM} at 150 °C (%)
PH1A	25	26.93 ± 0.56	20.35 ± 0.29	75.57	240	239.72 ± 5.87	161.01 ± 8.55	0.95 ± 0.02	0.95 ± 0.06
PH1B	25	19.75 ± 0.69	13.81 ± 1.14	69.92	240	129.86 ± 12.04	79.14 ± 8.98	0.65 ± 0.07	0.82 ± 0.13
		21.13 ± 0.55	15.76 ± 1.61	74.59		143.66 ± 13.50	102.19 ± 11.24	0.68 ± 0.08	0.81 ± 0.09
PH2	11	11.40 ± 0.92	6.01 ± 0.47	52.72	214	163.09 ± 19.71	81.76 ± 10.01	1.75 ± 0.13	2.05 ± 0.27
		11.03 ± 0.94	6.91 ± 0.96	62.65		114.35 ± 27.33	85.62 ± 13.87	1.40 ± 0.17	1.98 ± 0.46
PH3	24	22.08 ± 1.98	14.82 ± 1.23	67.12	300	292.88 ± 13.50	129.11 ± 19.54	1.57 ± 0.11	1.17 ± 0.04
		25.53 ± 2.41	17.29 ± 1.25	67.72		293.45 ± 35.03	156.16 ± 27.82	1.51 ± 0.15	1.15 ± 0.04
PH4	20	12.66 ± 0.58	7.87 ± 0.65	62.16	292	84.58 ± 22.67	69.06 ± 10.44	1.28 ± 0.43	1.98 ± 0.54
PH5	29	22.75 ± 0.97	15.25 ± 1.66	67.03	386	226.89 ± 27.31	156.43 ± 22.49	1.25 ± 0.14	1.27 ± 0.05
		25.39 ± 1.85	22.18 ± 1.12	87.36		273.70 ± 28.67	218.37 ± 11.88	1.21 ± 0.14	1.22 ± 0.18
VE1	15	11.63 ± 0.56	7.09 ± 0.30	60.96	325	255.45 ± 12.71	117.33 ± 4.81	2.53 ± 0.11	2.27 ± 0.19
		11.84 ± 1.02	7.92 ± 1.31	66.89		281.12 ± 21.17	133.00 ± 6.93	2.82 ± 0.10	2.09 ± 0.26
VE2	28	20.58 ± 1.98	12.02 ± 1.17	58.41	320	315.28 ± 40.10	106.05 ± 15.21	1.56 ± 0.15	1.40 ± 0.14
		20.15 ± 2.01	11.63 ± 1.41	57.72		274.26 ± 48.71	133.31 ± 18.54	1.46 ± 0.23	1.25 ± 0.11
VE3	20	16.52 ± 0.46	7.35 ± 1.11	44.49	424	357.82 ± 19.34	145.47 ± 16.41	2.84 ± 0.12	2.48 ± 0.11
		15.25 ± 0.90	7.43 ± 0.57	48.72		329.32 ± 61.26	134.43 ± 16.66	2.68 ± 0.37	2.46 ± 0.17
EP	27	36.72 ± 4.29	3.82 ± 0.99	10.40	484	561.30 ± 60.83	39.97 ± 3.64	1.91 ± 0.15	1.33 ± 0.06
		28.47 ± 3.44	5.47 ± 1.86	19.21		531.28 ± 16.34	38.62 ± 5.73	2.25 ± 0.33	1.09 ± 0.11
BMI	69	31.05 ± 6.48	26.28 ± 4.65	84.64	828	473.43 ± 69.59	432.37 ± 79.74	1.72 ± 0.20	1.81 ± 0.16
PEEK	40	39.92 ± 10.05	35.29 ± 12.31	88.40	656	655.56 ± 107.98	438.21 ± 82.57	2.03 ± 0.21	2.07 ± 0.52

*Please note that PH1A was injection moulded, while PH4, BMI and PEEK samples were tested only in one direction due to the higher processing pressure required a smaller mould tool; Ef – flexural modulus, σfM – flexural strength, εfM – flexural strain·

Table 3
Flexural properties of the moulded and post-cured phenolic samples in two orthogonal directions*.

Material	E_f data (GPa)	E_f at RT (GPa)	E_f at 150 °C (GPa)	E_f retained (%)	σ_{fM} data (MPa)	σ_{fM} at RT (MPa)	σ_{fM} at 150 °C (MPa)	ε_{fM} at RT (%)	ε_{fM} at 150 °C (%)
PH1A	25	26.10 ± 0.42	22.52 ± 0.31	86.28	240	245.22 ± 29.31	216.54 ± 9.48	0.96 ± 0.12	0.99 ± 0.04
PH1B	25	23.81 ± 0.46	20.71 ± 0.26	86.98	240	164.54 ± 15.01	126.99 ± 9.25	0.71 ± 0.07	0.64 ± 0.05
		21.92 ± 0.74	18.85 ± 1.39	85.99		140.99 ± 10.13	110.53 ± 17.11	0.65 ± 0.05	0.60 ± 0.09
PH2	11	11.46 ± 0.86	9.38 ± 0.68	81.85	214	114.59 ± 42.91	83.06 ± 11.53	1.07 ± 0.34	1.00 ± 0.09
		11.86 ± 0.88	9.53 ± 1.01	80.35		131.97 ± 29.20	96.43 ± 17.61	1.27 ± 0.21	1.16 ± 0.14
PH3	24	22.32 ± 1.28	19.10 ± 1.63	85.57	300	215.89 ± 33.62	170.11 ± 25.72	1.08 ± 0.19	1.00 ± 0.07
		26.28 ± 3.46	23.69 ± 0.96	90.14		255.83 ± 27.98	209.69 ± 14.19	1.08 ± 0.14	1.00 ± 0.08
PH4	20	11.53 ± 2.38	8.69 ± 2.14	75.37	292	96.74 ± 29.84	95.37 ± 29.41	1.49 ± 0.69	1.45 ± 0.27
PH5	29	23.23 ± 2.35	23.15 ± 1.45	99.66	386	231.96 ± 26.29	231.97 ± 14.16	1.16 ± 0.06	1.26 ± 0.16
		27.55 ± 3.48	27.25 ± 2.24	98.91		220.47 ± 62.96	196.28 ± 58.06	0.90 ± 0.14	0.83 ± 0.16

*Please note that PH1A and PH4 samples were tested only in one direction due to PH1A was injection moulded and PH4 required higher processing pressure in a smaller mould tool.
Ef – flexural modulus, σfM – flexural strength, εfM – flexural strain.

The filler generally enhances the modulus but also acts as stress concentrations and sites of crack initiation, leading to lower toughness in the composite samples [42,43].

The flexural modulus values of PH3 specimens only differ 5% in weft and 12% in warp direction. This is because the rovings were not perfectly arranged perpendicularly in the prepreg roll provided. The fibre tows in warp direction were 10–15° off resulting in lower flexural modulus values. However, the flexural strength was still within 5% in comparison with the datasheet in both directions.

PH4 and PH5 show nearly 40% and 12–20% lower flexural modulus than from the datasheet and around 70% and 30–40% lower flexural strength values, respectively. In both cases this is due to the different sample preparation method because to produce the data in the datasheet the specimens were net shape moulded by the manufacturer, which means higher fibre orientation in the resulting samples and a closed "moulded" surface with less flaws and weak points as discussed earlier.

The glass reinforced vinyl-ester based moulding compound samples (VE1 and VE3) have a flexural modulus at ambient between 11 and 16 GPa depending on the glass fibre content and around 20 GPa for the carbon reinforced moulding compound (VE2). Their flexural strength at ambient is around 250 and 360 MPa, which is comparable with PH3 (phenolic woven glass prepreg) under similar conditions. This is due to

the vinyl-ester based composites exceptional 3% strain at failure. However, their flexural modulus and flexural strength decrease by 55–60% at 150 °C. The epoxy based moulding compound (EP) exhibited a flexural modulus of over 30 GPa and the flexural strength around 550 MPa, which makes this material a competitive candidate at room temperature. However, at 150 °C there is a huge loss in performance with the flexural modulus is only 10–20%, while the flexural strength is only 7% of the ambient values. The flexural modulus and flexural strength obtained for BMI sample are only about half of the values from the datasheet. This is again due to the net shape moulded samples made by the manufacturer and then compared to machined ones in this study. While the results for PEEK samples were within 5% for both flexural modulus and flexural strength. Although the variation between individual specimens was 25% and 16%, respectively.

The flexural modulus values of the phenolic based moulding compounds stayed within 5% after the post-curing process at room temperature but were enhanced by 20–50% at 150 °C compared to as-moulded conditions. This also means that the retained flexural modulus values increased from 52-87% to 75–99% for the phenolic samples after the applied post-curing process. This shows that the post-curing profile used in this study was efficient in enhancing the properties of the phenolic moulding compounds at 150 °C.

It can be summarised that the post-curing process had a positive effect on the thermomechanical properties. It is also noteworthy that most industrial components are net-shape moulded in practice. However, post-machining (e.g. drilling holes, surface preparation, etc.) can cause surface flaws and might reduce properties, as discussed in this study. If further enhancement of stiffness is required, it can be achieved through optimised fibre alignment within the structure, where mechanical stiffness beyond randomly oriented fibre architectures are possible.

3.1.2. Comparison between injection and compression moulded samples

As a further comparison the Novalac type phenolic moulding compound with 35 wt% of chopped glass was also injection moulded (sample PH1A) with this compared to the results gained by compression moulding with the same material (PH1B), which also contains a substantial amount of mineral filler. The injection moulded parts (PH1A) have higher fibre alignment at the critical cross-section, therefore the measured flexural modulus in these samples was 30–40% higher. The inclusion of mineral fillers also causes embrittlement, both PH1A and PH1B failed at below 1% flexural strain. It can be also concluded that the flexural strength is nearly 80% higher for the injection moulded specimens (PH1A). This is thought to be due to closed sample surfaces in net-shape moulded samples – as produced via injection moulding, compared to the machined surfaces of samples cut from compression moulded plaques, where specimen surfaces are likely to contain flaws acting as crack initiations, resulting in failure at lower loads.

3.2. Dynamical mechanical analysis (DMA) test results

The glass transition temperatures from DMA test results are summarised in Table 4. As can be seen, the transition temperatures do not provide easily understandable data on the thermo-mechanical performance of the moulding compounds at higher temperatures. The glass transition of polymer materials is usually defined by the temperature at the inflection point (T_g) of the decrease in the storage modulus curve according to ISO 6721-11-2012 standard. However, other specific temperatures can be also defined, such as the temperature of the peak of the loss modulus (T_{loss}) and tangent delta ($T_{tan delta}$) curves or the temperature corresponding to the onset of the transition from glassy state, as determined by the intercept of two tangents in the storage modulus
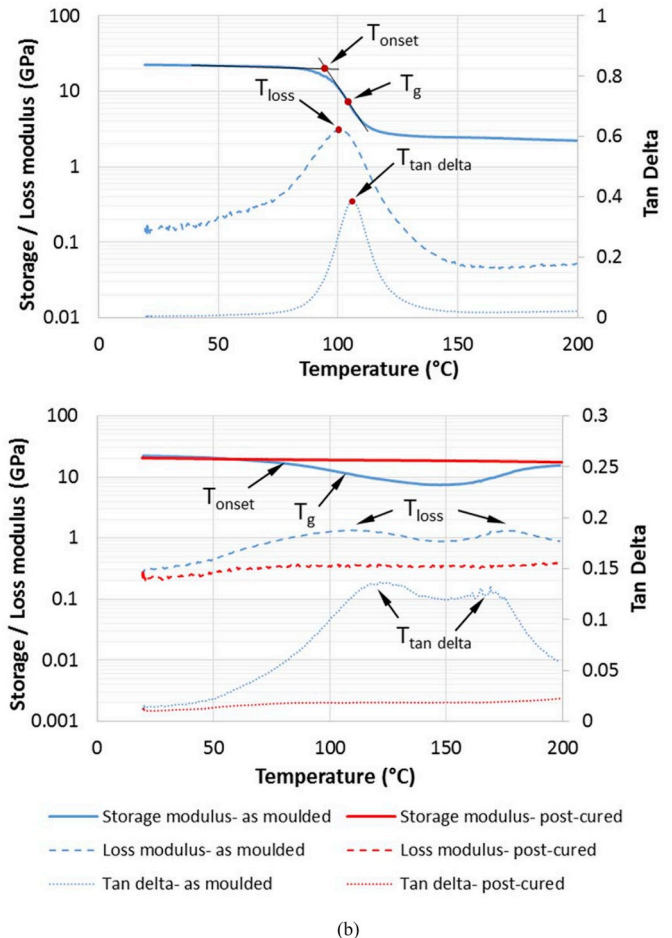

(b)

Fig. 3. Specific transition temperatures for epoxy (a) and PH3 before and after post-cure (b).

Table 4
Glass transition temperatures from DMA test results in two orthogonal directions.

Material	As moulded				Post-cured			
	T_{onset} (°C)	T_g (°C)	T_{loss} (°C)	$T_{tan delta}$ (°C)	T_{onset} (°C)	T_g (°C)	T_{loss} (°C)	$T_{tan delta}$ (°C)
PH1A	38/168	67/194	199	191	39/173	58/175	195	191
	40/169	75/178	194	194	124/187	126/>200	198	99/>200
PH1B	146	157	181	180	179	>200	193	>200
	143	163	189	186	149	>200	71/>200	76/>200
PH2	116	136	132/179	169	167	55/188	173	174
	119	140	149/176	162	42/182	59/>200	97/>200	102/>200
PH3	38	70	80/176	167	52/167	54/173	75/>200	100/>200
	41	69	81/180	167	41/175	50/>200	110/>200	118/>200
PH4	38/144	45/161	>200	49/122/>200	47/107/187	59/111/>200	61/>200	63/>200
	36/155	46/169	>200	51/>200	44/99/183	60/115/>200	58/>200	59/>200
PH5	31/193	45/90	141/>200	144/>200	110/121/160	120/144	>200	>200
	35/>200	48/>200	>200	133/>200		31/120/184	>200	>200
VE1	123	143	150	165	N/A	N/A	N/A	N/A
	129	154	159	166				
VE2	121	145	143	156	N/A	N/A	N/A	N/A
	122	145	144	157				
VE3	122	150	154	158	N/A	N/A	N/A	N/A
	120	151	152	156				
EP	89	102	101	106	N/A	N/A	N/A	N/A
	86	98	98	105				
BMI	174	>200 (215)	>200 (219)	>200 (241)	N/A	N/A	N/A	N/A
	168	191	>200≫	>200				
PEEK	127	149	151	159	N/A	N/A	N/A	N/A
	134	162	153	162				

curve (T_{onset}). These temperatures can be obtained for epoxy and vinyl-ester samples easily because each significant temperature occurs just once during the DMA test (Fig. 3a). However, in case of phenolics, these temperatures occurred twice or more due to the change in cross-linking density during post-curing (Fig. 3b). From the results in Table 4, it is evident that the transition temperatures do not provide easily understandable data on the thermo-mechanical performance of the moulding compounds at higher temperatures. Whilst Tg data is provided, the main parameter of interest in this paper was the dynamic storage modulus, which is an important property directly related to the material stiffness. Understanding the behaviour of this parameter at elevated temperatures can provide selection guidance in various structural applications. DMA results for all samples are summarised in Table 5. All materials examined, showed a fall in modulus at 150 °C as expected. For better understanding of the material behaviour at higher temperatures, a ratio was calculated based on the storage modulus values at ambient (23 °C) and at elevated temperature (150 °C), to provide a comparative data to the flexural test values discussed earlier (Eq. (1)). Fig. 4a shows the storage modulus-temperature curves for the phenolic based moulding compounds over the temperature range of interest. It should be noted that the initial stiffness values at ambient will differ in these samples, due to the differing fibre type, and volume fractions of each individual material type – as expected. The retained modulus of these phenolic moulding compounds at 150 °C is between 60 and 80%. Fig. 4b shows the behaviour of the same materials after a 16 h heat treatment at 180 °C. In all cases post-curing helped to dramatically improve stiffness retention of the phenolic moulding compounds. Fig. 4a shows PH3 experienced a significant drop until 130 °C, where it is thought, a post-curing process starts within its structure that results in increasing flexural storage modulus values. This is because phenolics are able to cross-link after their normal curing process due to the presence of active sites in their chain and therefore increasing the storage modulus [44]. Other phenolic samples (PH1A, PH1B and PH2) demonstrate similar effect but the characteristic drop in storage modulus starts at a higher temperature and the drop is not as significant compared to PH3. The initial large decrease in storage modulus can be significantly reduced with the 16 h heat treatment at 180 °C as can be seen in Fig. 4b. All the other post-cured phenolic moulding compounds show a gradual decrease in the storage modulus with increasing temperature. The retained modulus

of these phenolic materials at 150 °C is between 82 and 95%. The PH4 sample is uncharacteristically lower at around 70% (a repeat test gave identical behaviour for this sample). Comparing retained modulus data for all the composite systems tested (Table 5), post-cured phenolics are generally far better performing than vinyl-ester and epoxy based composites. Fig. 4c presented data for the other composite types tested. It is clear that the storage modulus values drop markedly for vinyl-ester samples (VE1, VE2 and VE3) above 120 °C. The retained modulus at 150 °C in all three cases varies between 42 and 50%, which means that these materials cannot be used successfully at this temperature. The graphs for vinyl-ester and epoxy also indicate that these materials cannot be post-cured in order to enhance their heat resistance, as evidenced by the continuous drop in modulus over the entire temperature range. The epoxy based moulding compound (EP) has a significant drop at an even lower temperature, ~90 °C, while its retained modulus at 150 °C is just around 10%. The storage modulus of the PEEK samples only starts decreasing at around 130 °C but the retained modulus at 150 °C is still between 75 and 91%. The storage modulus of the BMI sample gradually decreases until around 170 °C, where a slight drop in this property appears. Its retained modulus at 150 °C is over 85%. The advantage of using PEEK and BMI samples is that they do not require post-curing in order to be heat resistant. However, the BMI sample needs longer processing time (90 min) compared to the other materials. Also these materials are expensive and difficult to process, requiring higher processing temperatures and larger presses that need to be equipped with cooling, in order to speed processing time - which would in any event, be far slower and more energy intensive than processing via the phenolic route.

3.3. Relationship between flexural modulus (3 PB) and flexural storage modulus (DMA)

The mean flexural modulus values of the two orthogonal directions obtained from the three point bend testing were plotted against the corresponding flexural storage modulus data obtained from DMA tests for each material (Fig. 5a). When considering a vast difference in material type, fibre length volume fraction etc., Fig. 5a does show a general correlation between the two sets of results across this very varied sample range. However there is appreciable scatter in the data, which questions

Table 5
Flexural storage modulus values of the moulded and post-cured samples obtained from DMA tests in two orthogonal directions.

Material	E_f data (GPa)	As moulded			Post-cured		
		E_f' at RT (GPa)	E_f' at 150 °C (GPa)	E_f' retained (%)	E_f' at RT (GPa)	E_f' at 150 °C (GPa)	E_f' retained (%)
PH1A	25	27.13	18.26	67.31	26.73	22.41	83.84
		27.00	18.64	69.04	25.99	22.61	86.99
PH1B	25	20.56	12.55	61.04	18.26	15.76	86.31
		20.82	13.45	64.60	20.07	16.50	82.21
PH2	11	10.88	5.78	53.13	16.24	14.84	91.38
		11.54	6.97	60.40	10.21	8.58	84.04
PH3	24	22.28	7.49	53.13	19.84	18.69	94.20
		30.76	11.71	60.40	25.99	24.02	92.42
PH4	20	8.21	5.05	61.51	9.13	6.23	68.24
		11.10	7.10	63.96	15.12	10.95	72.42
PH5	29	13.18	10.28	78.00	14.50	13.18	90.90
		19.08	15.32	80.29	13.76	13.06	94.91
VE1	15	11.60	4.90	42.24	N/A	N/A	N/A
		13.70	6.90	50.36			
VE2	28	26.50	11.70	44.15	N/A	N/A	N/A
		17.20	7.50	43.60			
VE3	20	12.45	5.32	42.73	N/A	N/A	N/A
		13.81	6.27	45.40			
EP	27	22.48	2.46	10.94	N/A	N/A	N/A
		25.47	2.24	8.79			
BMI	69	17.26	14.80	85.74	N/A	N/A	N/A
		23.58	20.57	87.23			
PEEK	40	28.33	21.16	74.69	N/A	N/A	N/A
		46.70	42.58	91.18			

Ef'-flexural modulus, Ef'-flexural storage modulus.
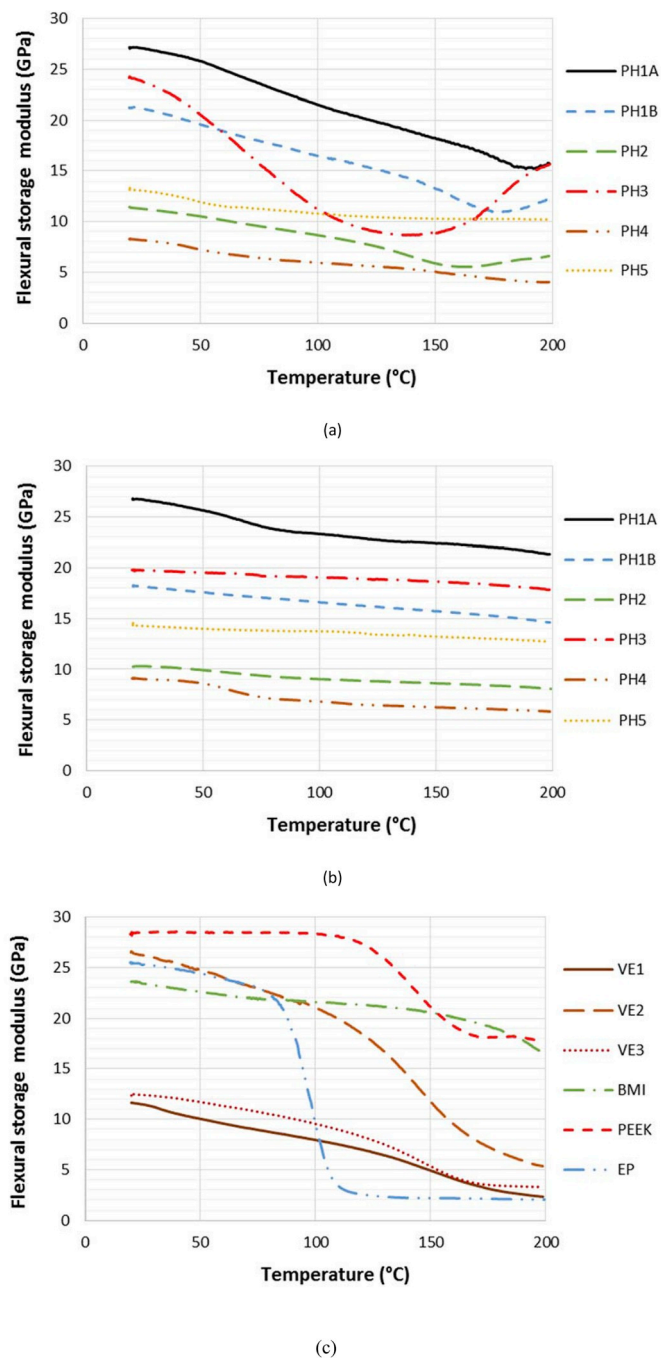
(a)

(b)

(c)

Fig. 4. Representative thermo-mechanical graphs of phenolic moulding compounds as compression moulded (a), than post-cured (b) and other resin based moulding compounds for comparison (c).

the validity of solely relying on DMA test data as an indicator of higher temperature performance in composites. On close examination of the data, it was realised that the most influential correlation factor was fibre length. The results were therefore arranged in to three different graphs according to various fibre lengths. The smaller fibre lengths, 3–6 and 12.5 mm, are in the same graph (Fig. 5b) showing good correlation with a linear trend between the two parameters. Fig. 5c shows the mid-range with 25 and 50 mm fibre length results. Here clearly there is far more scatter than in the samples and even the standard deviation values are higher than with shorter fibre lengths (Fig. 5b). The DMA results for the 25 mm samples are seen to be lower than parity (as evidenced by the number of results below the equity line on the graph). There are reasons

why the DMA results for this fibre length are systematically lower than the 3 PB. Firstly, the moulding compound is generally placed in the centre of the mould tool and then flows outwards to fill the mould, where fibre tows tend to align with the flow direction. Considering this, it is highly likely that almost all fibres will be misaligned with the sample length direction, and end up being cut somewhere. Secondly, it is argued that the 3 PB samples would very likely contain longer fibres purely because they are wider and longer than the DMA samples, where it is very unlikely that fibres would end up intact in the DMA sample. This effect is not apparent in continuous or the shorter fibres where both 3 PB and DMA would contain a similar distribution of fibre lengths. Fig. 5d shows results for continuous fibre samples. These results further strengthen the argument, in that good correlation is seen in the continuous fibre samples. However, the compression moulded specimens without post-curing process tested at 150 °C show lower values for the DMA test results. This is due to the intense drop in the flexural storage modulus with increasing temperature (Fig. 4a, PH3), while the post-curing process also starts below 150 °C. This means that the three point bending flexural specimens started to post-cure in the 150 °C heated chamber before the flexural test, resulted in higher flexural modulus values compared to the DMA test results at the same temperature. In Fig. 4a the flexural storage modulus increases from 7.49 to 11.71 to 15.54 and 20.90 GPa just over 15 min when the specimens were heated with 3 °C/min rate between 150 and 200 °C. In Fig. 5d this tendency is represented with red arrows showing that the flexural storage modulus values would have been higher at the same condition. This fact proves the point that post-curing is relevant in order to achieve suitable and reliable performance of the phenolic moulding compounds. PH1A, PH1B and PH2 samples started to post-cure above 150 °C, therefore there is little less difference seen observed in the three point bending tests at elevated temperature.

3.4. Micro computed tomography analysis

The micro-CT images of the DMA specimens with different fibre lengths are shown in Fig. 6. Whilst these scans are very sample-specific they do give information on the types of fibre distribution seen. Please note that only fibre tows can be seen in these images due to the resolution (38.7 μm pixel size). The 3–6 mm fibre length sample shows a homogenous distribution of the fibres (Fig. 6a) because no agglomerations are visible, which resulted less difference of the flexural modulus between the three point bending and DMA test results. The 12.5 mm fibre length sample show less even distribution of the fibre orientation but still looks randomised (Fig. 6b). However, the mid-range fibres, 25 mm (Figs. 6c) and 50 mm (Fig. 6d) as a tow occupying more space resulting in less random structure within the smaller DMA sample size. Another issue is the narrower DMA specimens would result in shorter fibre lengths generally in the DMA samples compared to the full size three point bending specimens. The sample contains continuous fibres (Fig. 6e) show that the fibres running through the spans and the perpendicular fibres have no effect on the flexural modulus but situated with a slight angle (~10°) from perpendicular. Furthermore, higher magnification images (7.1 μm pixel size) reveal the difference in general flow pattern in the 3–6 mm fibre length samples. The injection moulded sample, PH1A (Fig. 7a) shows more orientation in longitudinal direction of the specimen (the injection direction) compared to the compression moulded alternative, PH1B (Fig. 7b). This alignment results in higher stiffness of the PH1A part as discussed earlier in this paper.

3.5. Material selection guide

In this section the most relevant results are summarised and discussed further. The aim is to provide guidance in composite material selection especially for automotive designers that makes an important addition to existing digital design libraries [45]. The flexural modulus and strength of the materials were normalised with density in order to
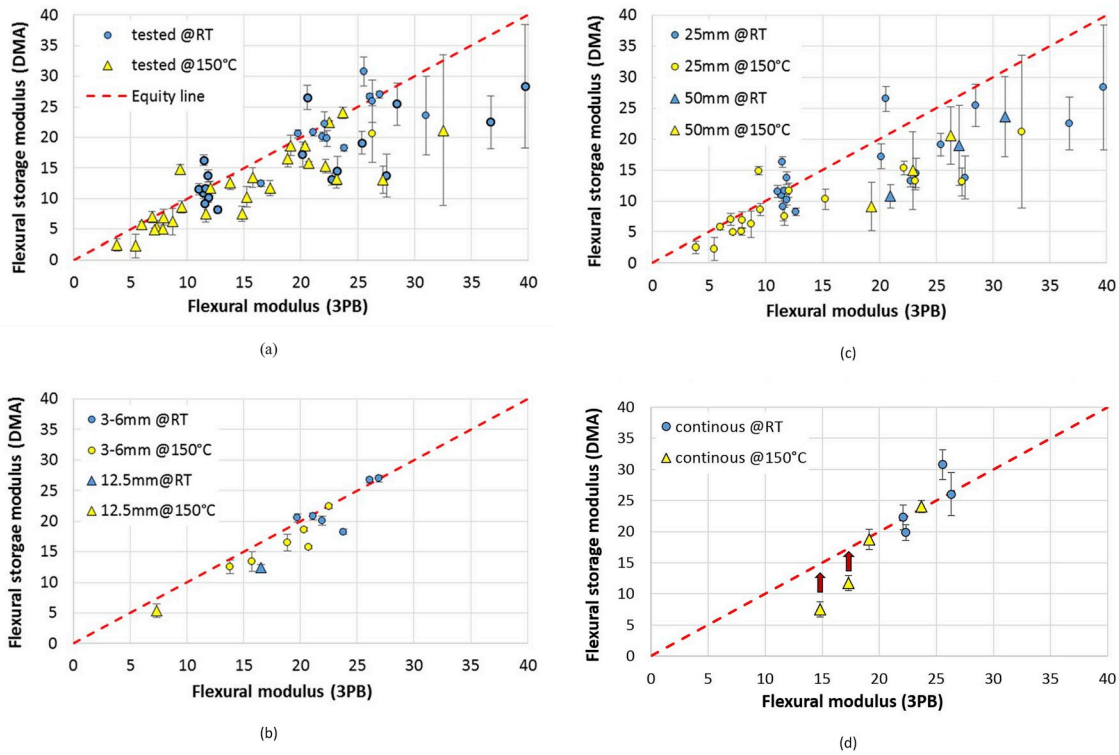
Fig. 5. Mean values of flexural moduli from three point bending with standard deviation vs flexural storage moduli from DMA tests results including all the tests carried out (a) and separated by fibre length: 3–6 mm and 12.5 mm (b); 25 and 50 mm (c); and continuous (d).
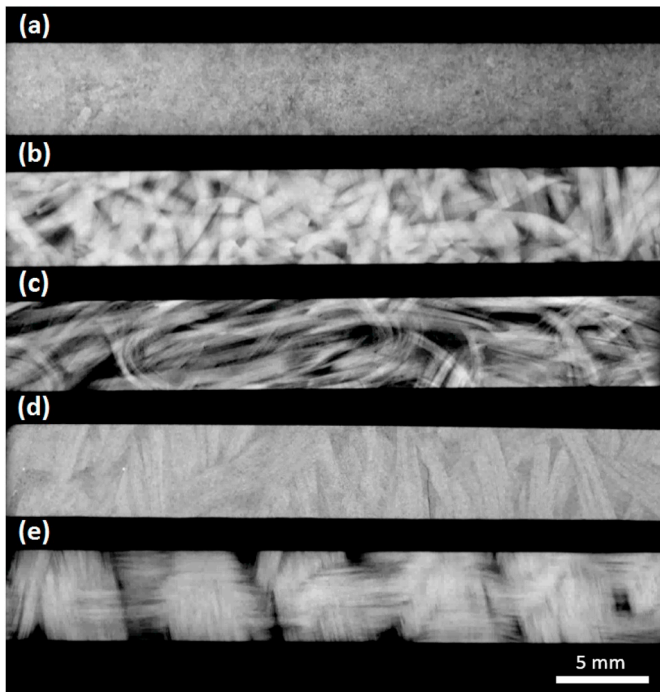

Fig. 6. Representative micro-CT images from the DMA specimens with different fibre lengths, 3–6 mm, PH1B (a) 12.5 mm, VE3 (b); 25 mm, PH2 (c); 50 mm, BMI (d) and continuous, PH3 (e).

Fig. 7. Fibre orientation of the 3–6 mm fibre length samples as injection moulded, PH1A (a) and compression moulded, PH1B (b).

room temperature the epoxy based moulding compound (EP) has high values of both the specific flexural modulus and strength, while the vinyl-ester based samples (VE) have higher specific strength than stiffness values, which is due to their exceptional 3% strain at failure.

The PEEK and BMI samples can provide outstanding flexural properties even at higher temperatures. It can be seen that PEEK lost more strength than stiffness at elevated temperature, and BMI had more balanced loss in both properties at the same conditions. However, their costly manufacturing process and raw material prices make them less attractive for automotive engineers at the moment.

The phenolic moulding compounds represent a group, where the flexural properties are maintained even at higher temperatures, whilst the raw material cost is much lower than the PEEK and BMI composites. From the tested samples PH5 shows the best specific properties due to its
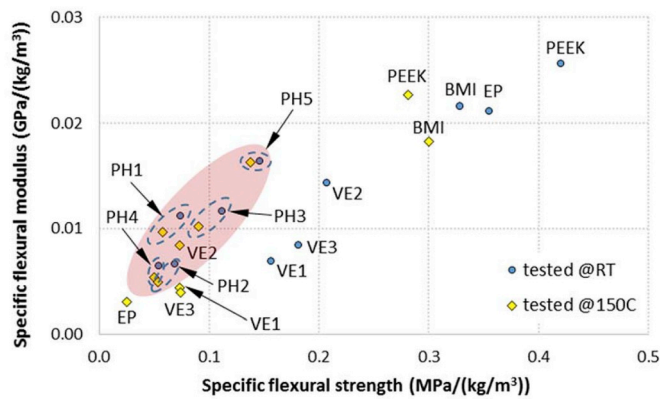
get a specific value and plotted against each other in Fig. 8 for better visualisation.

From the tests discussed earlier, and with the help of the graph, it is obvious that vinyl-ester and epoxy based moulding compounds cannot be successfully applied at elevated temperatures, close to 150 °C. At

Fig. 8. The relationship between the specific flexural modulus and strength of the selected moulding compounds based on their mean values.

Fig. 9. The theoretical flexural modulus (achievable maximum value based on manufacturers datasheet) plotted against relative cost of the materials, price based on 10 tons of minimum order from the material and normalised with the current market price of aluminium as a benchmark.

carbon reinforced structure, which makes this sample also lighter than the other phenolic moulding compounds used in this study. PH3 follows with the second highest specific strength and modulus due to its high fibre content and their alignment in a biaxial woven structure. PH1 is just behind showing less difference in the flexural modulus compared to PH3, which is due to the high filler content. On the other hand this makes its structure more brittle as discussed earlier and reduces the strength. PH2 and PH4 has similar properties due to their close glass content and randomised structure. However, their properties can be improved with more alignment applied in a specific direction.

The significance of cost is just as important as the material properties when selecting materials. To ensure that material selection is guided in this study, the theoretical flexural modulus at room temperature (obtained from material datasheets provided by the manufacturers) was plotted against cost of the materials in Fig. 9. In order to take into account the influence of inflation and eliminate issues due to various currencies a relative cost per unit volume was defined by Eq. (2) similar to CES Edupack [46].

$$C_{V,R} = \frac{(Cost\ of\ material/\ kg)\ x\ (Density\ of\ material)}{(Cost\ of\ aluminium/\ kg)\ x\ (Density\ of\ aluminium)} \qquad (2)$$

The graph shows that generally, cost increases linearly with flexural moduli. However, the position on the graph of some materials shifted in the up and left direction, which means that the same flexural modulus can be achieved at lower raw material cost (PH1, PH3, VE2 and EP). Of course this does not mean directly that the flexural strength will be acceptable in all cases, or that this property will be maintained at higher temperatures. For example PH1 can be used at lower load values and limited deformation, if strength of the material is not as critical as rigidity and PH3 can withstand higher deformations due to its longer fibre lengths.

4. Conclusions

This study provides important additional information and test data describing and comparing the stiffness performance of a wide range of commercially available composite systems, at ambient and 150 °C; data not routinely available in manufacturers datasheets but vital in specifying such materials for many emerging composite applications, particularly within the automotive sector. The study introduces the concept of "retained modulus" presenting this as a better way to compare relative performance at elevated temperatures, providing a more meaningful guide to designers and engineers than the glass transition temperatures itself. The study showed that phenolic based composites are highly resilient to thermally induced modulus loss, performing far better than the vinyl-esters and epoxy based systems. Post-curing was very effective at further improving and stabilising
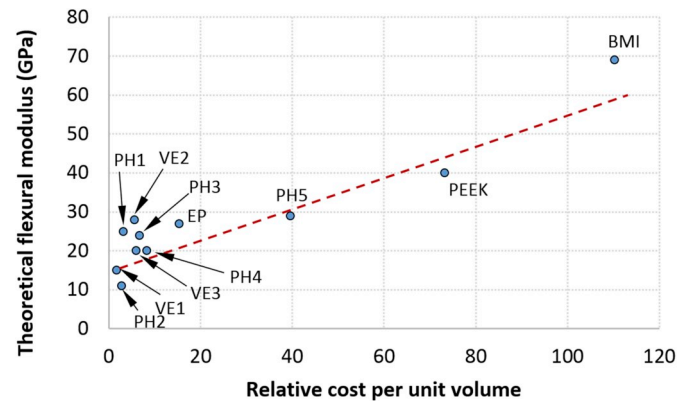
retained modulus in all phenolic systems. The study also compared DMA results with three point bending test data where uniquely, tests were performed both at ambient and 150 °C. Cross-comparison of the results from the two techniques showed that, whilst there is the same general correlation between measurements, DMA in isolation should not be relied upon as an assessment of stiffness performance at elevated temperature. DMA measurements were shown to be generally lower compared to three point bending data, in composite samples containing similar fibre lengths to the length of typical DMA samples. However, the two methods show moderately good agreement where fibre length equals or is lower than 12.5 mm and for continuous reinforcement. PEEK and BMI thermoplastic composites were found to demonstrate the highest retained modulus of the materials tested, however the downsides in terms of cost and manufacturing complexity would hinder their utility in large volume manufacturing applications at the present state. Furthermore, a material selection guide in this study was aiming to help researchers to choose appropriate materials for their work and to provide information for deeper understanding on the commercially available moulding compounds.

Appendix A. Supplementary data

Supplementary data to this article can be found online at https://doi.org/10.1016/j.compositesb.2019.106921.

References

[1] Edwards T. Composite materials revolutionise aerospace engineering. Ingenia 2008;36:24–8. http://www.ingenia.org.uk/getattachment/Ingenia/Issue-36/Composite-materials-revolutionise-aerospace-engine/Edwards.pdf.

[2] Mangalgiri PD. Polymer-matrix composites for high-temperature applications. Defence Sci J 2005;55(2):175–93.

[3] Tadini P, Grange N, Chetehouna K, Gascoin N, Senave S, Reynaud I. Thermal degradation analysis of innovative PEKK-based carbon composites for high-temperature aeronautical components. Aerosp Sci Technol 2017;65:106–16.

[4] Stewart R. Composites help lightweight the automotive market. Mater Today 12 Mar 2009. https://www.materialstoday.com/composite-applications/features/composites-help-lightweight-the-automotive-market/.

[5] Anon. "Light under the bonnet". The Engineer; 11 Aug 2003. https://www.theengineer.co.uk/issues/8-August-2003/light-under-the-bonnet/.

[6] Mazumdar S. Opportunity and challenges in automotive composites industry. Lucintel; 12 Dec 2013. http://www.lucintel.com/lucintelbrief/lucintel-brief-opportunity-and-challenges-in-automotive-composites-industry.pdf.

[7] Tröster S. Composites parts for automotive internal combustion engines. Fraunhofer Institute for Chemical Technology; 13 Apr 2015. http://www.jeccomposites.com/knowledge/international-composites-news/composites-parts-automotive-internal-combustion-engines.

[8] Lattimer BY, Ouellette J, Trelles J. Thermal response of composite materials to elevated temperatures. Fire Technol 2011;47(4):823–50.

[9] Lielens G, Pirotte P, Couniot A, Dupret F, Keunings R. Prediction of thermomechanical properties for compression moulded composites. Compos Part A 1998; 29(1–2):63–70.

[10] Kumarasamy S, Shukur Zainol Abidin M, Abu Bakar MN, Nazida MS, Mustafa Z, Anjang A. Effects of high and low temperature on the tensile strength of glass fiber reinforced polymer composites. In: IOP conference series: materials science and engineering, vol. 370; 2018. p. 012021. 1.

[11] Kuchera NK, Samusenkob AA. Assessment of elasticity characteristics and strength parameters of unidirectional polymer composites at high temperatures. Strength Mater 2017;49(3):136–48.

[12] Danil'chuk EL, Kucher KA, Kushnarev AP, Potapov AM, Rudnitskii NP, Samusenko AA, Filatov VE. Deformation and strength of unidirectional carbonfiber-reinforced plastics at elevated temperatures. Strength Mater 2015;47(4): 573–8.

[13] Chen Y, Chen P, Hong C, Zhang B, Hui D. Improved ablation resistance of carbon–phenolic composites by introducing zirconium diboride particles. Compos Part B 2013;47:320–5.

[14] Bahramian AR, Kokabi M, Famili MHN, Beheshty MH. Ablation and thermal degradation behaviour of a composite based on resol type phenolic resin: process modeling and experimental. Polymer 2006;47(10):3661–73.

[15] Park J-M, et al. Effects of carbon nanotubes and carbon fiber reinforcements on thermal conductivity and ablation properties of carbon/phenolic composites. Compos Part B 2014;67:22–9.

[16] Patton RD, Pittman Jr CU, Wang L, Hill JR, Day A. Ablation, mechanical and thermal conductivity properties of vapor grown carbon fiber/phenolic matrix composites. Compos Part A 2002;33(2):243–51.

[17] Ding J, et al. Improved high-temperature mechanical property of carbon-phenolic composites by introducing titanium diboride particles. Compos Part B 2019;157: 289–94.

[18] Ding J, et al. Thermal stability and ablation resistance, and ablation mechanism of carbon–phenolic composites with different zirconium silicide particle loadings. Compos Part B 2018;154:313–20. 2018.

[19] Luo C, Des Jardin PE. Thermo-mechanical damage modeling of a glass–phenolic composite material. Compos Sci Technol 2007;67(7–8):1475–88.

[20] Koizumi K, Charles T, De Keyser H. Phenolic moulding compounds. In: Pilato L, editor. Phenolic resins: a century of progress. Berlin, Heidelberg: Springer; 2010. p. 383–437.

[21] Mouritz AP, Mathys Z. Mechanical properties of fire-damaged glass-reinforced phenolic composites. Fire Mater 2000;24(2):67–75.

[22] Hirano K, Asami M. Phenolic resins—100 years of progress and their future. React Funct Polym 2013;73(2):256–69.

[23] Brady P, Brady M. Automotive composites: which way are we going? Reinforc Plast 2007;51(10):32–5.

[24] Wheatley A, Warren D, Das S. Development of low-cost carbon fibre for automotive applications. Adv Compos Mater Automot Appl: Struct Integr Crashworthiness 2014;1:51–73.

[25] Forintos N, Czigany T. Multifunctional application of carbon fiber reinforced polymer composites: electrical properties of the reinforcing carbon fibers – a short review. Compos Part B 2019;162:331–43.

[26] Shirshova N, et al. Structural composite supercapacitors. Compos Part A 2013;46: 96–107.

[27] Li Y, et al. Experimental study of damage characteristics of carbon woven fabric/ epoxy laminates subjected to lightning strike. Compos Part A 2015;79:164–75.

[28] Baker DA, Rials TG. Recent advances in low-cost carbon fiber manufacture from lignin. J Appl Polym Sci 2013;130(2):713–28.

[29] Balakrishnan VS, Seidlitz H. Potential repair techniques for automotive composites: a review. Compos Part B 2018;145:28–38.

[30] Palmer J, Savage L, Ghita OR, Evans KE. Sheet moulding compound (SMC) from carbon fibre recyclate. Compos Part A 2010;41:1232–7.

[31] Yao S-S, et al. Recent advances in carbon-fiber-reinforced thermoplastic composites: a review. Compos Part B 2018;142:241–50.

[32] Summerscales J, Short D. Carbon fibre and glass fibre hybrid reinforced plastics. Composites 1978;9(3):157–66.

[33] Markovic S, Dunjic B, Zlatanic A, Djonlagic J. Dynamic mechanical analysis study of the curing of phenol-formaldehyde novolac resins. J Appl Polym Sci 2001;81(8): 1902–13.

[34] Da-Peng Z, Hong F. Mechanical and high-temperature properties of glass fibers reinforced phenolic composites. J Reinf Plast Compos 2008;27(13):1449–60.

[35] Bindu RL, Reghunadhan Nair CP, Ninan KN. Phenolic resins with phenyl maleimide functions: thermal characteristics and laminate composite properties. J Appl Polym Sci 2001;80(10):1664–74.

[36] Yao Y, Zhao T, Yu Y. Novel thermosetting resin with a very high glass-transition temperature based on bismaleimide and allylated novolac. J Appl Polym Sci 2005; 97(2):443–8.

[37] Guo Z-S, Feng J, Wang H, Hu H, Zhang J. A new temperature-dependent modulus model of glass/epoxy composite at elevated temperatures. J Compos Mater 2013; 47(26):3303–10.

[38] Orgéas L, Dumont PJJ. Sheet molding compounds. In: Nicolais L, Borzacchiello S, editors. Wiley encyclopedia of composites. Wiley; 2011. p. 2683–718.

[39] Evans AD, Qian CC, Harper LT, Warrior NA, Brookbank P, Savage L. Flow characteristics of carbon fibre sheet moulding compounds. In: Proceedings of 20th international conference on composite materials. Copenhagen: July; 2015. p. 10.

[40] Harper LT, Turner TA, Warrior NA, Rudd CD. Characterisation of random carbon fibre composites from a directed fibre preforming process: the effect of fibre length. Compos Part A 2006;37(11):1863–78.

[41] Ratna D. Handbook of thermoset resins. Shawbury, UK: ISmithers; 2009.

[42] Lee J, Yee AF. Fracture of glass bead/epoxy composites: on micro-mechanical deformations. Polymer 2000;41(23):8363–73.

[43] Shirinbayan M, et al. Mechanical characterization of a low density sheet molding compound (LD-SMC): multi-scale damage analysis and strain rate effect. Compos Part B 2017;131:8–20.

[44] Kuzak SG, Shanmugham A. Dynamic mechanical analysis of fiber-reinforced phenolics. J Appl Polym Sci 1999;73(5):649–58.

[45] Ramalhete PS, Senos AMR, Aguiar C. Digital tools for material selection in product design. Mater Des 2010;31(5):2275–87.

[46] Ashby M. CES Edupack 2010, 2 material and process selection charts Copyright Granta Design Ltd. http://www.grantadesign.com/download/pdf/teaching_resource_books/2-Materials-Charts-2010.pdf.